Frequency-specific mechanism links human brain networks for spatial attention

Amy L. Daitch[a,1], Mohit Sharma[a], Jarod L. Roland[b], Serguei V. Astafiev[c], David T. Bundy[a], Charles M. Gaona[a], Abraham Z. Snyder[c,d], Gordon L. Shulman[c], Eric C. Leuthardt[a,b,2], and Maurizio Corbetta[c,d,e,2]

[a]Department of Biomedical Engineering, [b]Department of Neurological Surgery, [c]Department of Neurology, [d]Department of Radiology, and [e]Department of Anatomy and Neurobiology, Washington University in St. Louis, St. Louis, MO 63110

Edited by Marcus E. Raichle, Washington University in St. Louis, St. Louis, MO, and approved October 21, 2013 (received for review April 29, 2013)

Selective attention allows us to filter out irrelevant information in the environment and focus neural resources on information relevant to our current goals. Functional brain-imaging studies have identified networks of broadly distributed brain regions that are recruited during different attention processes; however, the dynamics by which these networks enable selection are not well understood. Here, we first used functional MRI to localize dorsal and ventral attention networks in human epileptic subjects undergoing seizure monitoring. We subsequently recorded cortical physiology using subdural electrocorticography during a spatial-attention task to study network dynamics. Attention networks become selectively phase-modulated at low frequencies (δ, θ) during the same task epochs in which they are recruited in functional MRI. This mechanism may alter the excitability of task-relevant regions or their effective connectivity. Furthermore, different attention processes (holding vs. shifting attention) are associated with synchrony at different frequencies, which may minimize unnecessary cross-talk between separate neuronal processes.

One of the hallmarks of effective behavior is the ability to flexibly attend to particular stimuli in the environment. Selective attention can be driven endogenously by one's current goals or by salient external stimuli. Human neuroimaging studies have identified two sets of fronto-parietal regions that are recruited during these two types of attention. A set of dorsal fronto-parietal regions (dorsal attention network or DAN) shows sustained activity during endogenous or goal-driven attention (1), and reorienting to unexpected targets transiently activates both the DAN and a second set of regions, the ventral attention network (VAN) (2). Although functional MRI (fMRI) has identified the brain regions that are involved in these attentional operations (3, 4), the slow nature of the hemodynamic response has severely limited the study of network dynamics at behaviorally relevant time scales (5). Here, we report results obtained by cortical surface (electrocorticography or ECoG) recordings in epilepsy patients undergoing clinical monitoring to identify seizure foci. Electrode locations for each subject were colocalized with functional brain networks, including the DAN and VAN identified in the same subjects using fMRI. This experimental paradigm allowed us to objectively link fast electrophysiological dynamics, during performance of an attention task, to well-studied functional brain networks.

ECoG measures nonspiking, local field potential oscillations across a range of frequencies, which are thought to reflect fluctuations in local neuronal excitability (6, 7). Phase modulations of activity within a region and between regions may therefore affect, respectively, their ability to respond to inputs and to transfer information between one another (8, 9). In support of this theory, previous studies in both animals and humans have shown that either local or long-distance synchrony change in a task-specific manner; for example with visual attention, sensory-motor integration, or working memory (10–17).

In this study, we examine whether task-specific modulations of synchrony occur during a well-characterized spatial attention (Posner) task in both task-relevant (DAN, VAN, sensory-motor) and irrelevant (default-mode) networks previously identified with fMRI. We predicted that attending to a spatially cued location or reorienting to the location of an unexpected target would produce selective phase modulations within and synchronization within and between task-relevant but not task-irrelevant networks based on fMRI.

Results

Posner Spatial Orienting Task. Seven invasively monitored patients performed a version of the Posner spatial cueing task, a standard paradigm for studying attention to spatial locations. Subjects were cued with a central arrow (500 ms) to attend to the side of the monitor where an upcoming target was likely to appear. After a brief (500 ms) delay, a rotated "L" or "T" was presented peripherally on the cued side (80% of trials, "valid"), or the uncued side (20% of trials, "invalid") of the monitor. Subjects were asked to respond as quickly and accurately as possible with one of two mouse buttons to indicate the target identity (Fig. 1). On average, subjects performed the task with 90.1% accuracy. One outlier subject only responded correctly 75.6% of the time, so we eliminated this subject's data from subsequent analyses. The remaining six subjects responded with 92.5% accuracy on average (range: 85.8–97.2%), and all of them responded faster to valid than invalid targets (paired t test, $P < 0.05$, across subjects). Subject-specific behavioral results are presented in Tables S1 and S2.

Significance

Humans have the remarkable ability to flexibly attend to stimuli in the environment and seamlessly shift behaviors, depending on sensory conditions and internal goals. Neuroimaging studies have shown that tasks involving particular cognitive domains consistently recruit specific broadly distributed functional brain networks. A fundamental question in neuroscience is how the brain flexibly manages communication within and between these brain networks, allowing task-relevant regions to interact while minimizing the influence of task-irrelevant activity. In this report we show that low-frequency neuronal oscillations, which reflect fluctuations in neuronal excitability, are modulated selectively within task-relevant, but not -irrelevant brain networks. This modulation of oscillatory activity may coordinate the selective routing of neuronal information within the brain during everyday behavior.

Author contributions: A.L.D., G.L.S., E.C.L., and M.C. designed research; A.L.D., M.S., J.L.R., S.V.A., D.T.B., and C.M.G. performed research; A.L.D. and A.Z.S. contributed new reagents/analytic tools; A.L.D. analyzed data; and A.L.D., G.L.S., E.C.L., and M.C. wrote the paper.

The authors declare no conflict of interest.

This article is a PNAS Direct Submission.

[1]To whom correspondence should be addressed. E-mail: adaitch@wustl.edu.

[2]E.C.L. and M.C. contributed equally to this work.

This article contains supporting information online at www.pnas.org/lookup/suppl/doi:10.1073/pnas.1307947110/-/DCSupplemental.

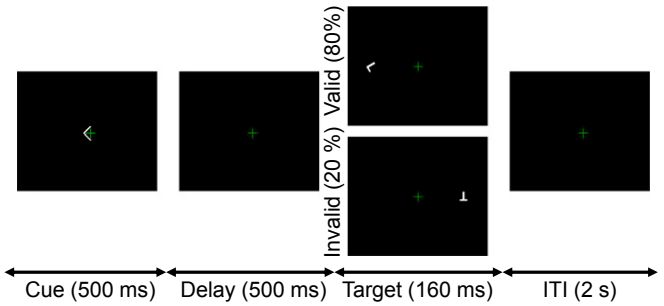

Fig. 1. Posner spatial cueing task.

We focused our analyses on neural activity during two periods. First, following the cue, spatial attention is directed toward the location at which the upcoming target is expected to appear (voluntary orienting). Second, following presentation of an invalid target, attention must be disengaged from the cued side and redirected to the other side of the monitor (stimulus-driven reorienting). The DAN and VAN play specific, well-documented roles in voluntary and stimulus-driven orienting of attention, and both are recruited during particular epochs of the Posner task. The DAN is recruited following both the cue and the presentation of an invalid target, whereas the VAN is inactive following the cue but responds strongly to invalid targets.

fMRI Definition of Resting-State Networks. Before electrode implantation, resting-state fMRI scans were obtained, allowing us to identify both the DAN and VAN in each subject using standard functional connectivity analyses. Similar analyses identified a sensorimotor network (SMN), which prepares and executes the subjects' response to the target, and a default-mode network (DMN) in which activity is either unchanged or suppressed during performance of visual attention tasks (18, 19). The ECoG electrodes were spatially registered with the fMRI data, allowing us to assign specific electrodes to each of the four networks (see *Experimental Procedures* and *SI Experimental Procedures* for further details). Recording individual fMRI data allowed us to localize distributed networks that have variable topography across subjects (Fig. S1*A*). Classifying electrodes based on distance from atlas-defined seeds (<20 mm from seed) missed 77.5% of electrodes classified as part of a network based on individual functional connectivity maps, suggesting that collecting individual fMRI data are advantageous for network classification of electrodes in individuals. Fig. S1*B* shows the electrode locations for the subjects in this study.

Phase Modulations During Voluntary Spatial Attention. Our first set of analyses looked at whether particular events within the task induce phase modulations over brain regions expected to be engaged during those epochs. We computed intertrial coherence (ITC) at single electrodes, a measure that reflects the consistency, across trials, of oscillatory phase at a particular frequency and latency (Fig. S2 *A* and *B*).

Following the central cue, subjects must orient and maintain covert attention to the location where they expect the target to appear. Fig. 2*A* exhibits example time-frequency ITC plots time-locked to the cue in a single subject; Fig. 2*B* shows group-averaged ITC time-courses in the δ- and θ-bands, averaged across electrodes within each functional network. Following the cue, most electrodes over the DAN and SMN exhibited increased ITC in the δ-band (1–3 Hz), which was maintained throughout the cue and delay periods, in a manner consistent with the role of these regions in orienting and motor planning (Fig. 2 *A* and *B*). The DAN also exhibited a more transient increase in ITC following the cue in the θ-band (3–7 Hz) (Fig. 2*B*). Conversely, few electrodes over the VAN or the DMN, regions which are not expected to be involved in endogenous orienting, exhibited an increase in ITC following the cue (Fig. 2 *A* and *B*).

Because an increase in ITC following a stimulus may reflect a stimulus-evoked response, we also computed changes in δ and θ power following the cue. A stimulus-evoked response (i.e., an additional signal superimposed on the ongoing oscillations) will manifest as both an increase in ITC and power following the stimulus, whereas a pure phase-resetting of ongoing oscillations will manifest as an increase in ITC with no accompanying power change or a power decrease. We found that few electrodes exhibiting significant δ ITC during the cue or delay also exhibited a significant increase in δ power, and many exhibited a δ power decrease (Fig S3 *A–C*). Furthermore, there was no significant correlation between the magnitude of δ ITC and δ power increase during either the cue or delay period (Fig. S3*D*). Therefore, although we can't rule out a stimulus-evoked explanation for δ ITC, we believe the increase in δ ITC following the cue at least partially reflects phase-resetting of spontaneous oscillations in task-relevant networks. The θ ITC, on the other hand, was accompanied more prevalently by an increase in θ power. Additionally, θ power and θ ITC were significantly positively correlated during the cue period (Fig. S3 *A–D*), suggesting that the transient increase in θ ITC following the cue more likely reflects a stimulus-evoked response.

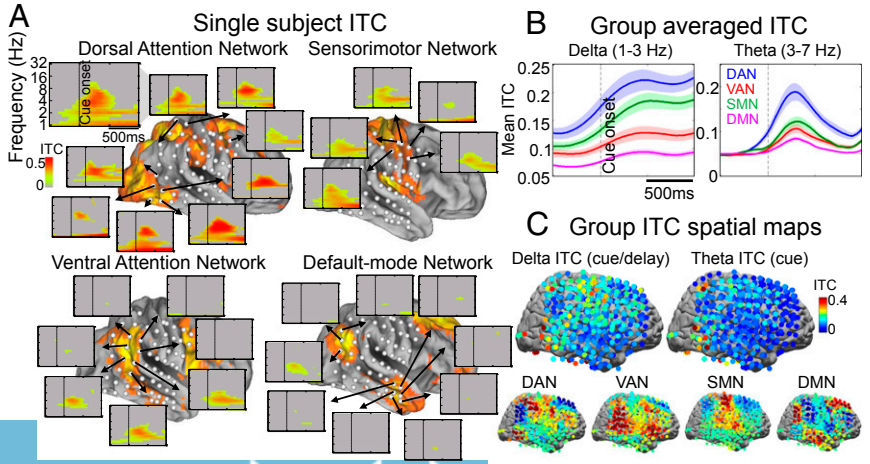

Fig. 2. Phase resetting in task-relevant regions following endogenous cue. (*A*) ITC plots around cue onset (dotted line), over electrodes in the DAN, VAN, SMN, and DMN, in an exemplar patient (thresholded at Rayleigh test, $P < 0.001$, uncorrected; nonsignificant values are greyed out). (*B*) ITC averaged over electrodes in each functional network (across patients) in two frequency bands; δ (1–3 Hz), and θ (4–7 Hz). Shaded regions represent SEMs. (*C*) Spatial distribution of ITC in the δ-band during the cue and delay period across all subjects (*Upper Left* brain plot), and spatial distribution of ITC in the θ-band during the cue period (*Upper Right* brain plot), along with the four functional connectivity networks of interest in this study (Fisher *z*-transformed correlation values), sampled at the electrode coordinates across all subjects (*Lower*; see *General Methods* for details on generating functional connectivity network maps). Electrodes were all projected onto a single hemisphere.

As a more data-driven approach, unbiased by the fMRI definition of networks, we also plotted the spatial distribution of ITC in the δ- and θ-bands across all electrodes and subjects, during the same epochs where we observed ITC increases in Fig. 2*B*, the cue and delay periods for δ, and the cue period for θ (Fig. 2*C*). The map of δ ITC during the cue and delay periods is spatially significantly positively correlated with the DAN and SMN functional connectivity maps, significantly negatively correlated with the DMN, and not significantly correlated with the VAN (DAN: $r = 0.2861$, $P < 1e\text{-}4$; SMN: $r = 0.1094$, $P = 0.0202$; DMN: $r = -0.1595$, $P = 0.0007$). The map of θ cue period ITC is significantly positively correlated with the DAN ($r = 0.1988$, $P < 1e\text{-}4$) but not significantly correlated with any of the other three functional networks studied. Thus, both analyses show that the topography of phase modulation lines up well with task-relevant functional connectivity networks.

Patterns of Phase-Resetting Following Cue Carry Spatial Information About Locus of Attention. To better isolate neural signals related to orienting and maintaining attention to a spatial location, we compared the activity following right vs. left cues, or more specifically cues contralateral vs. ipsilateral to the electrode locations. DAN and the visual cortex are known to exhibit spatial selectivity, responding more strongly when attention is directed contralaterally (4, 20). Therefore, we expected greater phase-modulatory activity at these regions following contralateral vs. ipsilateral cues, particularly right around target onset, possibly to increase the excitability of brain regions selective for the attended location. Furthermore, because the stimulus-evoked response to the cue is matched for left vs. right cues, this comparison allowed us to test more specifically whether phase-related modulations reflect phase-resetting of ongoing activity. Indeed several electrodes over visual occipital and DAN regions exhibited greater ITC following contralateral vs. ipsilateral cues throughout the cue and delay period (Fig. 3). Notably, the difference in ITC increased throughout the delay period, peaking around target onset. Spatial selectivity was not observed in the DMN or VAN (Fig. 3*B*). Spatially selective modulations did not reflect eye movements to the cued location (Fig. S4*A*).

In summary, δ phase-resetting occurs bilaterally in DAN and the visual cortex, but also shows relative contralateral spatial selectivity that peaks close to target onset. Interestingly, this pattern, including spatial selectivity in task-relevant networks and its time-course, and absence in VAN and DMN, closely matches patterns of fMRI activity on the same paradigm (20, 21).

Resetting of θ-Phase When Reorienting to Unexpected Stimulus. In 20% of trials, subjects had to shift attention to a target in the unattended location to make a discrimination response. To isolate activity corresponding to these stimulus-driven shifts of attention, we compared neural responses following invalid vs. valid targets. Fig. 4*A* shows examples ITC time-frequency plots time-locked to target onset, separated by invalid and valid targets, at electrodes over the DAN and VAN in a single subject. Following invalid targets, electrodes over both the DAN and VAN exhibited significantly greater ITC than during valid trials, primarily in the θ- band (3–7 Hz). Fig. 4*B* shows the corresponding group-averaged ITC time-courses in the θ-band. This reorienting response was stronger in the right hemisphere, in agreement with the fMRI literature (2, 18, 22) (Fig. 4*C* and Fig. S5). No significant reorienting response was observed in the SMN or DMN (Fig. 4*B*), areas not expected to be involved in stimulus-driven reorienting.

Again, as a more data-driven approach, we created spatial maps of the difference in θ ITC between invalid and valid targets across all electrodes and subjects, separately for the right and left hemispheres (Fig. 4*C*). This spatial map of the difference in θ ITC between invalid and valid targets is positively correlated with the VAN in both the right and left hemispheres, although

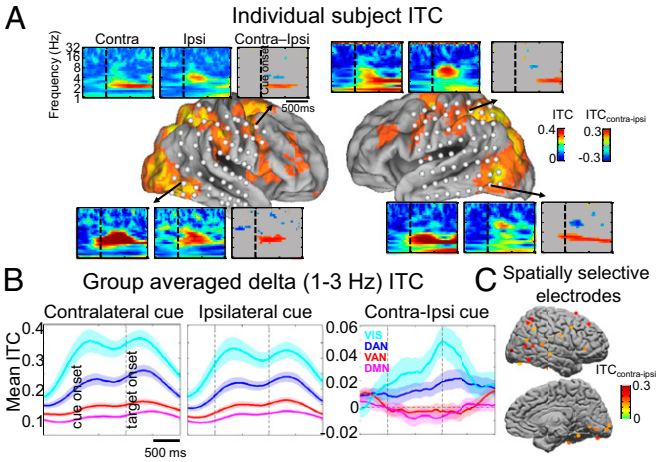

Fig. 3. Spatial specificity of phase-resetting response. (*A*) ITC plots at electrodes over the DAN in two patients following a contralateral cue (relative to electrode positions), ipsilateral cue, and the difference between the two conditions (thresholded at permutation test $P < 0.05$, uncorrected). (*B*) The δ-band ITC time-courses over electrodes in the DAN, visual, and DMN, averaged across all electrodes in all patients. Visual electrodes were defined as those in the occipital cortex that exibited a transient γ-power increase after the presentation of the cue or target stimuli. At the group level, the DAN and visual networks exhibited a significant effect of cue direction on δ ITC that peaked around the time of target onset (paired *t* test during delay, DAN: $P = 0.0115$, Visual: $P = 0.0016$). Shaded regions represent SEMs. (*C*) Locations of electrodes exhibiting significantly greater δ (2 Hz) ITC at target onset following contralateral versus ipsilateral cues (permutation test, $P < 0.01$, uncorrected).

more strongly correlated in the right hemisphere (right VAN: $r = 0.3199$, $P < 1e\text{-}4$; left VAN: $r = 0.1423$, $P = 0.0189$). It is important to note that the stimuli are identical during valid and invalid trials, allowing us to attribute differences between these two conditions to attention-related processes, not to sensory stimuli. This θ-band reorienting response also cannot be explained by eye movements to unexpected targets (Fig. S4*B*). Thus, both our stimulus-driven and goal-driven attention analyses support our prediction that phase-modulatory activity is topographically aligned with brain networks known to be involved in these cognitive processes.

Phase Synchronization Within and Between Task-Relevant Networks. In addition to phase modulations at individual electrodes, we predicted that phase differences between regions should facilitate communication between task-relevant but not -irrelevant regions (Fig. S2*C*). We addressed this issue in two ways. First we computed phase-locking values (PLV) between every pair of electrodes, with the expectation that task-relevant but not -irrelevant electrodes would become more phase-locked throughout the course of the task. Phase-locking is a measure reflecting the consistency of the phase difference between two oscillatory signals of similar frequencies. Because brain oscillations aren't pure sinusoids, two unrelated brain signals should exhibit randomly distributed phase differences across time. High PLV over time is therefore suggestive of an interaction between two regions. We computed the PLV between all electrode pairs, both within and between networks, during consecutive 500-ms epochs of the task: the intertrial interval (ITI) (500 ms before cue onset), cue presentation, delay, and target presentation (500 ms, starting at target onset). We focused our analysis on 2-Hz activity in the δ-band, where we found a peak in ITC during the delay (Fig. S6). We found that electrodes over the task-relevant DAN and SMN became more phase-locked with each other in the δ-band through the task, relative to the ITI, both within and between networks (paired *t* test,

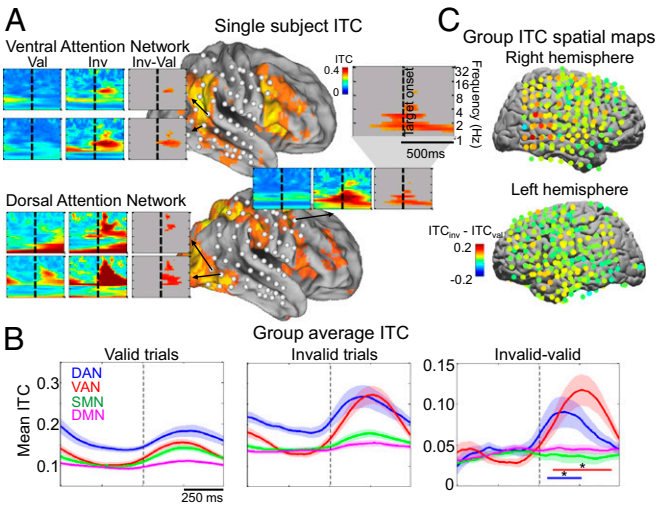

Fig. 4. Phase-resetting in task-relevant regions during stimulus-driven shifts of attention. (*A*) ITC plots around target onset (dotted line), for valid and invalid targets, over electrodes in the DAN and VAN in an exemplar patient, as well as the difference in ITC between invalid and valid trials (thresholded at permutation test $P < 0.01$, uncorrected). (*B*) ITC around target onset, averaged over electrodes in each functional network (across patients) in the θ-band, for valid trials, invalid trials, and the difference between the two conditions. Starred epochs mark time points when electrodes in a non-DMN network exhibit a significantly greater reorienting response than the DMN. Only DAN and VAN electrodes from the right hemisphere were included in this analysis, whereas both right and left hemisphere electrodes were included for the SMN and DMN. Shaded regions represent SEMs. (*C*) Spatial distribution of the difference in θ-band ITC following invalid vs. valid targets (averaged within the 500 ms following target onset) for both the right and left hemispheres.

$P < 0.01$, Bonferroni-corrected). On the other hand, electrodes over the task-irrelevant VAN became less phase-locked with each other over the course of the task, relative to the ITI (paired *t* test, $P < 0.01$, Bonferroni-corrected) (Fig. 5*A*). Fig. 5*B* shows example PLV maps in a single subject between a seed over frontal eye fields (FEF, marked in white) and every other electrode in the grid, computed around 2 Hz, during different epochs of the task. Note that during the ITI, phase-locking is mostly local, whereas during the trial, FEF becomes more phase-locked with other task-relevant electrodes over the middle temporal region, intraparietal sulcus, and motor cortex (see Fig. S7 for additional PLV maps with different seeds in two subjects). PLVs were also computed at higher frequencies; however, there were no significant increases in PLV between any network pairs during the delay period compared with the ITI in these higher frequencies, which is when activity related to sustained attention would be observed (Fig. S8*A*).

One potential concern with comparing PLVs within and between networks is that close pairs of electrodes tend to exhibit higher PLVs than distant pairs of electrodes, because of volume conduction, and electrode pairs within a given network are likely closer than electrode pairs between networks. To avoid this potential confound, we computed PLV changes between different epochs but the same electrode pairs, such that interelectrode distances were held constant between conditions. To ensure that PLV change (percent change in PLV between each epoch and the ITI) did not exhibit a distance effect, we plotted the PLV change versus interelectrode distance for all electrode pairs, and electrode pairs within each network. Fig. S8*B* shows that within each network, the largest PLV increases from the ITI to task epochs tended to occur between more distant electrodes (~40–80 mm). Furthermore, in task-relevant networks (DAN, SMN), there was a positive correlation between PLV change and interelectrode distance (Fig. S8*C*), indicating that on average larger PLV increases occurred between more distant electrodes.

Given that the period of the low-frequency oscillations at which ITC was observed here (~1–7 Hz; 140- to 1,000-ms period) is very long compared with the approximate conduction delay between connected regions (~10 ms) (23), we predicted that task-relevant regions should be approximately in phase at the frequencies where significant ITC was observed (Fig. S2*C*). Within the δ-band, the phase values at electrodes in the DAN and SMN, but not the DMN, were tightly clustered during the task (Fig. 6*A*). Furthermore, the average phase difference between the DAN and SMN decreased during the task (Fig. 6 *B* and *C*). This finding supports the idea that patterns of oscillatory activity may selectively enable task-relevant regions to interact during a task.

Discussion

Selective attention relies on the filtering of incoming sensory information in accordance with task demands, thought to result from the biasing of sensory brain regions by higher-order brain regions. Distributed brain networks recruited during endogenous or stimulus-driven attention have been localized with noninvasive human neuroimaging; however, the low temporal resolution of these methods has prevented investigations of the fast dynamics during attentional processes. Here we show that functional networks recruited during different forms of spatial attention based on fMRI studies (i.e., DAN for voluntary orienting; DAN and VAN for stimulus-driven reorienting) show task-specific phase-modulatory activity and synchronization, consistent with their postulated roles. These results suggest that one mechanism of selection in our task was the modulation of low-frequency rhythms, which presumably altered the excitability at single sites or the effective connectivity between task-relevant regions. The link between human neuroimaging and electrophysiology is notable because much of what we know about the neural correlates of attention comes from neuroimaging in human and electrophysiology in nonhuman primates (1, 24).

Neural Correlates of Phase Reset or Phase Synchronization. It is important to understand how the metrics we report in our results (ITC and PLV) reflect underlying neural dynamics both within and between brain regions. ITC refers to oscillatory activity at a single site that is phase-locked to an event within the task (i.e., has a consistent phase relationship to an event, across trials). This

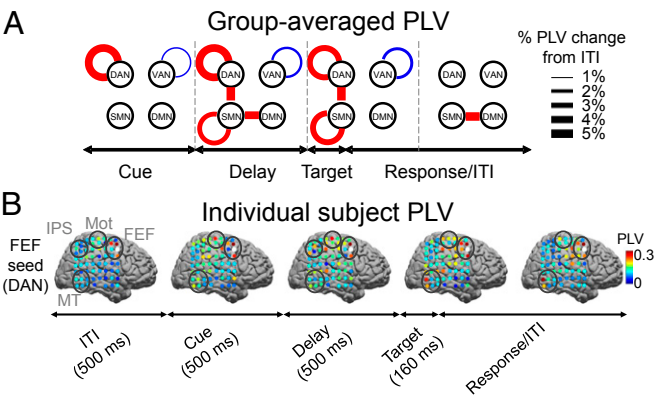

Fig. 5. δ (2 Hz) phase-locking within and between networks across task. (*A*) Percent change in PLV between different epochs of the task and the ITI, averaged across electrode pairs either within or between networks. Red lines represent increases in PLV from the ITI and blue lines represent decreases from the ITI. The thickness of each line is proportional to the percent PLV change. (*B*) Maps of PLV between a seed electrode over FEF (colored white) and all other electrodes in a single patient, across different task epochs. IPS, intraparietal sulcus; MT, middle temporal region.

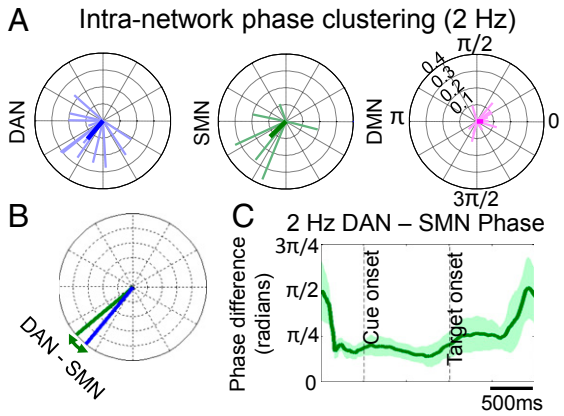

Fig. 6. Phase-clustering within and between task-relevant and -irrelevant networks. (*A*) Faded lines represent average phases across trials of individual electrodes, weighted by each electrode's ITC at that frequency and time point, from electrodes over the DAN, SMN, and DMN in a single patient at 2 Hz, at a time point during the delay period. Dark lines represent the interelectrode average. The angle of the resultant vector is the average phase across the group of electrodes and the magnitude relates to the degree of clustering between the electrodes. Note that the 2-Hz phases at DAN and SMN electrodes are much more tightly clustered than the phases at DMN electrodes. (*B*) Differences between the average DAN and average SMN phases, for the same subject and time point considered in *A*. (*C*) Phase difference between average DAN and average SMN phases, over the time course of a trial.

phase-locked activity may arise either because of an external stimulus or an endogenous source. ITC can also reflect either an additive signal superimposed on ongoing oscillations or phase-resetting of the ongoing oscillations themselves. Here, we not only showed that task-relevant brain regions became simultaneously phase-modulated (Figs. 2–4), but that they became more in phase with each other during the task (Fig. 6). More direct evidence for task-dependent synchronization between task-relevant regions comes from the analysis of PLV, which reflects the phase consistency between regions over time. Consistent with the ITC results, we showed that electrodes over task-relevant networks became more phase-locked with each other during the Posner task trial, relative to the ITI (Fig. 5). Task-irrelevant electrodes/networks (e.g., in the DMN), on the other hand, showed weak to no phase modulation during the task. We suggest that the observed network-specific phase modulations reflect enhanced excitability at or effective connectivity between task-relevant brain regions.

The spatial selectivity of phase-resetting in DAN and visual regions that contain topographic maps (25–27) also suggests that phase modulations may be important not only for linking different regions of a network, but also for selecting specific neuronal populations (e.g., neurons coding for left vs. right locations) within a network.

Although our surface recordings are unable to determine underlying brain structures that may bring about this synchrony, other anatomical studies, primarily in monkeys, suggest potential neural substrates. The pulvinar nucleus of the thalamus, for example, has broadly distributed cortical connections [most direct cortico-cortico connections have a parallel indirect path through the pulvinar (28)] and exhibits both attention-modulated spike rate (29) and synchrony with visual areas (30). The inhibitory thalamic reticular nucleus, which receives overlapping projections from prefrontal cortex and higher-order sensory cortical areas, may also play a role in modulating incoming sensory information with selective attention (15, 31, 32).

Frequency-Specific Phenomena with Two Types of Attention. One key aspect of our results is that phase modulations occurred in different frequency bands depending on the network and the relevant task process (Figs. 2 and 4, and Fig. S6). Sustained δ-phase modulations were observed in the DAN, SMN, and visual areas during the cue and delay periods, while maintaining attention to the cued location and preparing for a motor response (Figs. 2 and 3). In contrast, transient phase resetting in the θ-band occurred in the DAN and VAN following invalid targets (Fig. 4*B*), when subjects reoriented attention to the unexpected target.

The δ-phase at stimulus onset has been shown to correlate both with the magnitude of a sensory response and reaction time to a stimulus (33), suggesting that δ-phase relates to the level of local neuronal excitability. The δ-oscillations can also entrain to the rhythm of a task when it is predictable, such that stimuli arrive at a particular oscillatory phase, for example that corresponding to maximum excitability (33). In our study, ITC during the delay peaked at 2 Hz (Fig. S6), which has a cycle of 500 ms, the exact duration of the delay period. In two subjects, who also performed a version of the Posner task with a variable delay between the cue and target, the δ ITC was not sustained during the delay period, as it was with a constant delay (Fig. S9). This result suggests that when the cue–target interval is fixed, δ-oscillations may phase-reset, such that target onset aligns with the phase of maximal excitability.

Previous work has shown that θ-phase modulates γ power (7, 34), and γ activity has been associated with active sensory processing (14, 35). Furthermore, stronger θ phase-reset with saccades during exploration of a stimulus has been associated with better subsequent recall of that stimulus (36). Thus, the θ phase-reset we observe following invalid targets may allow for optimal sensory processing of the unexpected stimulus.

We do not claim that the δ- and θ-frequencies at which phase modulations are observed in this paradigm are associated specifically with endogenous and stimulus-driven attention. Likely, the oscillations modulated by a task are determined by many factors, including the temporal structure of a task (33) and the distribution of brain regions recruited (37). However, the observation that phase-resetting occurred at multiple frequencies simultaneously, in some cases on the same electrode, suggests that synchrony across multiple frequencies is a potential mechanism to allow multiple neuronal processes to occur simultaneously without interference.

Although the main attention effects reported here are in the low-frequency δ- and θ-bands, several previous studies of visual attention have shown coherence at higher frequencies (β, γ) (14, 38–40). In some of these earlier studies, neurons were driven continuously with visual stimuli, and thus attention was not purely endogenous. These studies also had a randomized cue–target interval, making phase entrainment to the stimuli impossible, whereas our study had a fixed delay between the cue and target. Low-frequency oscillations have been shown to entrain to the rhythm of a task, when stimuli are presented in a rhythmic, predicable manner (33). On the other hand, γ synchrony, which enhances the efficacy of communication between regions (41), but which is more metabolically costly than low-frequency activity (42), may operate under conditions of temporal uncertainty (43). Notably, both the pulvinar and thalamic reticular nucleus, mentioned above as a potential generators of cortical synchronous activity, operate in both phasic (i.e., transient) and tonic (i.e., sustained) modes (29, 32). These two modes may underlie the low frequency [shown here (15)] versus sustained high-frequency coherence (14, 39) correlates of attention, respectively.

Conclusions

We emphasize three conclusions. First, phase-resetting as measured with ECoG was observed in electrodes involved in particular cognitive functions as predicted by neuroimaging. The striking correspondence between ECoG and blood-oxygen level-dependent signals measured with fMRI not only provides electrophysiological support for the distinction between dorsal

and ventral attention networks, but also validates our approach of using neuroimaging data to predict the functional properties of specific electrodes.

Second, our results support the view that modulations in low-frequency oscillatory activity during a task may alter the excitability at or effective connectivity between functionally relevant regions within and between networks. Increased ITC in task-relevant networks was accompanied by both an increase in phase-locking and a tighter clustering of phase values within and between task-relevant networks, consistent with enhanced communication among those regions.

Finally, task-related changes in synchronization were frequency-specific, in agreement with work showing that different frequency scales in the cortical physiology are associated with different cognitive processes or brain states (6, 44). The δ-frequency modulations were associated with endogenous maintenance of spatial attention in the DAN and SMN, whereas more transient shifts of attention involved θ-phase modulations in both the DAN and VAN. Frequency-specific synchronization may link neuronal populations at different temporal scales and allow simultaneous interactions between different sets of networks/brain regions without interference, as in amplitude modulation (AM) radio broadcasting, where signals from different stations are carried on radio waves of different frequencies.

Experimental Procedures

Subjects. Seven patients with drug-resistant epilepsy participated in this study; all were undergoing surgery at Barnes Jewish Hospital in St. Louis for seizure mapping via ECoG before resection of their epileptic foci. All subjects provided informed consent before participating, which had been reviewed and approved by the Washington University School of Medicine Institutional Review Board. Electrode locations were determined purely for clinical reasons and thus varied from patient to patient. Fig. S1*B* illustrates the approximate electrode locations for the patients who participated in this study.

General Methods. During the monitoring phase of this procedure, in which brain activity was recorded from the implanted electrodes, subjects performed a version of the Posner spatial cueing task, described earlier. We allowed at least 2 d for subjects to recover from the surgery/anesthesia before having them perform the task. Before the surgery to implant the electrodes, resting-state fMRI scans were obtained for each subject (to generate functional connectivity network maps), and were used to localize brain regions of interest for the ECoG analysis. Postoperative CT scans (with electrodes) were also obtained to enable coregistration of electrode coordinates with the fMRI data, unless otherwise noted otherwise in *SI Experimental Procedures*.

Detailed data analysis methods are included in *SI Experimental Procedures*.

ACKNOWLEDGMENTS. We thank all the patients who participated in this study for their time. This work was supported by the James S. McDonnell Foundation; the Doris Duke Foundation; National Institute of Mental Health Grant R01 MH 71920-09; National Institute of Health Grants 5T32EY013360-10, UL1 TR000448, and TL1 TR000449; and the National Science Foundation NSF EFRI-1137211.

1. Corbetta M, Shulman GL (2002) Control of goal-directed and stimulus-driven attention in the brain. *Nat Rev Neurosci* 3(3):201–215.
2. Corbetta M, Patel G, Shulman GL (2008) The reorienting system of the human brain: From environment to theory of mind. *Neuron* 58(3):306–324.
3. Kastner S, Pinsk MA, De Weerd P, Desimone R, Ungerleider LG (1999) Increased activity in human visual cortex during directed attention in the absence of visual stimulation. *Neuron* 22(4):751–761.
4. Hopfinger JB, Buonocore MH, Mangun GR (2000) The neural mechanisms of top-down attentional control. *Nat Neurosci* 3(3):284–291.
5. Logothetis NK (2008) What we can do and what we cannot do with fMRI. *Nature* 453(7197):869–878.
6. Buzsáki G, Draguhn A (2004) Neuronal oscillations in cortical networks. *Science* 304(5679):1926–1929.
7. Lakatos P, et al. (2005) An oscillatory hierarchy controlling neuronal excitability and stimulus processing in the auditory cortex. *J Neurophysiol* 94(3):1904–1911.
8. Varela F, Lachaux JP, Rodriguez E, Martinerie J (2001) The brainweb: Phase synchronization and large-scale integration. *Nat Rev Neurosci* 2(4):229–239.
9. Fries P (2005) A mechanism for cognitive dynamics: Neuronal communication through neuronal coherence. *Trends Cogn Sci* 9(10):474–480.
10. Bressler SL, Coppola R, Nakamura R (1993) Episodic multiregional cortical coherence at multiple frequencies during visual task performance. *Nature* 366(6451):153–156.
11. Sarnthein J, Petsche H, Rappelsberger P, Shaw GL, von Stein A (1998) Synchronization between prefrontal and posterior association cortex during human working memory. *Proc Natl Acad Sci USA* 95(12):7092–7096.
12. Rodriguez E, et al. (1999) Perception's shadow: Long-distance synchronization of human brain activity. *Nature* 397(6718):430–433.
13. von Stein A, Chiang C, König P (2000) Top-down processing mediated by interareal synchronization. *Proc Natl Acad Sci USA* 97(26):14748–14753.
14. Fries P, Reynolds JH, Rorie AE, Desimone R (2001) Modulation of oscillatory neuronal synchronization by selective visual attention. *Science* 291(5508):1560–1563.
15. Lakatos P, et al. (2009) The leading sense: Supramodal control of neurophysiological context by attention. *Neuron* 64(3):419–430.
16. Siegel M, Donner TH, Oostenveld R, Fries P, Engel AK (2008) Neuronal synchronization along the dorsal visual pathway reflects the focus of spatial attention. *Neuron* 60(4): 709–719.
17. Saleh M, Reimer J, Penn R, Ojakangas CL, Hatsopoulos NG (2010) Fast and slow oscillations in human primary motor cortex predict oncoming behaviorally relevant cues. *Neuron* 65(4):461–471.
18. Corbetta M, Kincade JM, Ollinger JM, McAvoy MP, Shulman GL (2000) Voluntary orienting is dissociated from target detection in human posterior parietal cortex. *Nat Neurosci* 3(3):292–297.
19. Shulman GL, et al. (2003) Quantitative analysis of attention and detection signals during visual search. *J Neurophysiol* 90(5):3384–3397.
20. Sylvester CM, Shulman GL, Jack AI, Corbetta M (2007) Asymmetry of anticipatory activity in visual cortex predicts the locus of attention and perception. *J Neurosci* 27(52):14424–14433.
21. Sylvester CM, Shulman GL, Jack AI, Corbetta M (2009) Anticipatory and stimulus-evoked blood oxygenation level-dependent modulations related to spatial attention reflect a common additive signal. *J Neurosci* 29(34):10671–10682.
22. Shulman GL, et al. (2010) Right hemisphere dominance during spatial selective attention and target detection occurs outside the dorsal frontoparietal network. *J Neurosci* 30(10):3640–3651.
23. Buzsaki G (2006) *Rhythms of the Brain* (Oxford Univ Press, New York, NY).
24. Desimone R, Duncan J (1995) Neural mechanisms of selective visual attention. *Annu Rev Neurosci* 18:193–222.
25. DeYoe EA, et al. (1996) Mapping striate and extrastriate visual areas in human cerebral cortex. *Proc Natl Acad Sci USA* 93(6):2382–2386.
26. Sereno MI, Pitzalis S, Martinez A (2001) Mapping of contralateral space in retinotopic coordinates by a parietal cortical area in humans. *Science* 294(5545):1350–1354.
27. Silver MA, Kastner S (2009) Topographic maps in human frontal and parietal cortex. *Trends Cogn Sci* 13(11):488–495.
28. Saalmann YB, Kastner S (2011) Cognitive and perceptual functions of the visual thalamus. *Neuron* 71(2):209–223.
29. Petersen SE, Robinson DL, Keys W (1985) Pulvinar nuclei of the behaving rhesus monkey: Visual responses and their modulation. *J Neurophysiol* 54(4):867–886.
30. Saalmann YB, Pinsk MA, Wang L, Li X, Kastner S (2012) The pulvinar regulates information transmission between cortical areas based on attention demands. *Science* 337(6095):753–756.
31. Zikopoulos B, Barbas H (2006) Prefrontal projections to the thalamic reticular nucleus form a unique circuit for attentional mechanisms. *J Neurosci* 26(28):7348–7361.
32. Zikopoulos B, Barbas H (2007) Circuits formultisensory integration and attentional modulation through the prefrontal cortex and the thalamic reticular nucleus in primates. *Rev Neurosci* 18(6):417–438.
33. Lakatos P, Karmos G, Mehta AD, Ulbert I, Schroeder CE (2008) Entrainment of neuronal oscillations as a mechanism of attentional selection. *Science* 320(5872):110–113.
34. Canolty RT, et al. (2006) High gamma power is phase-locked to theta oscillations in human neocortex. *Science* 313(5793):1626–1628.
35. Womelsdorf T, Fries P, Mitra PP, Desimone R (2006) Gamma-band synchronization in visual cortex predicts speed of change detection. *Nature* 439(7077):733–736.
36. Jutras MJ, Fries P, Buffalo EA (2013) Oscillatory activity in the monkey hippocampus during visual exploration and memory formation. *Proc Natl Acad Sci USA* 110(32):13144–13149.
37. von Stein A, Sarnthein J (2000) Different frequencies for different scales of cortical integration: From local gamma to long range alpha/theta synchronization. *Int J Psychophysiol* 38(3):301–313.
38. Buschman TJ, Miller EK (2007) Top-down versus bottom-up control of attention in the prefrontal and posterior parietal cortices. *Science* 315(5820):1860–1862.
39. Gregoriou GG, Gotts SJ, Zhou H, Desimone R (2009) Long-range neural coupling through synchronization with attention. *Prog Brain Res* 176:35–45.
40. Saalmann YB, Pigarev IN, Vidyasagar TR (2007) Neural mechanisms of visual attention: How top-down feedback highlights relevant locations. *Science* 316(5831):1612–1615.
41. Tallon-Baudry C (2009) The roles of gamma-band oscillatory synchrony in human visual cognition. *Front Biosci* 14:321–332.
42. Schroeder CE, Lakatos P (2009) The gamma oscillation: Master or slave? *Brain Topogr* 22(1):24–26.
43. Schroeder CE, Lakatos P (2009) Low-frequency neuronal oscillations as instruments of sensory selection. *Trends Neurosci* 32(1):9–18.
44. Gaona CM, et al. (2011) Nonuniform high-gamma (60–500 Hz) power changes dissociate cognitive task and anatomy in human cortex. *J Neurosci* 31(6):2091–2100.